

Hidden-charm strong decays of the spin-2 partner of $X(3872)$

Gurjav Ganbold^{1,2,*} and M. A. Ivanov^{1,†}

¹*Bogoliubov Laboratory of Theoretical Physics, Joint Institute for Nuclear Research, 141980 Dubna, Russia*

²*Institute of Physics and Technology, Mongolian Academy of Sciences, 13330 Ulaanbaatar, Mongolia*

Hidden-charm strong decays of the spin-2 partner $X_2(4014)$ of the charmonium-like state $X(3872)$ have been studied in the framework of the covariant confined quark model. The exotic state X_2 has been interpreted as a four-quark state with molecular-type interpolating current. We have considered the decay widths of X_2 on the level of two-petal quark loops. The partial widths of the strong decays $X_2 \rightarrow \omega J/\Psi$ and $X_2 \rightarrow \rho^0 J/\Psi$ have been calculated and the related branching ratio has been analyzed.

PACS numbers: 13.20.Gd, 13.25.Gv, 14.40.Rt, 14.65.Fy, 14.40.Lb, 13.40.Hq, 12.39.-x, 12.38.Aw, 14.65.Dw

I Introduction

During the last two decades, a large number of new mesonic structures was discovered in the course of experimentally establishing the heavy hadron spectrum. The positions of many of them in the mass spectrum, quantum numbers, and decay widths seem to not fit the predictions of the conventional quark models of mesons (quark-antiquark pairs) and baryons (three-quark structures). These 'exotic' states are commonly referred to as XYZ states.

The massive amount of data accumulated over the past years on XYZ states makes the theoretical study of exotic hadrons with 'charm' quarks an essential tool for analyzing quantum chromodynamics at the confinement scale. Nowadays, a debate is ongoing between theoretical models about the nature of XYZ hadrons, and assumptions about different multiquark configurations have been developed to explain their properties, such as mass, decay width, and the main quantum numbers (for reviews see, e.g., Refs. [1–5]).

The first member of the XYZ family, the $X(3872)$ state in the charm sector was observed by the Belle collaboration in 2003 as a structure in the $\pi^+\pi^-J/\psi$ invariant mass spectrum [6]. Later, the LHCb Collaboration in 2013 determined its quantum numbers $J^{PC} = 1^{++}$ [7]. The $X(3872)$ is located very close to the $D\bar{D}^*$ threshold, and to date, $X(3872)$ is naturally considered as a shallow bound mesonic molecule ($D\bar{D}^*$) with quantum numbers $J^{PC} = 1^{++}$ (see, e.g. Refs. [8–12]).

Furthermore, the $X(3872)$ is often used as a basis for predicting possible exotic states due to the achievement of its molecular picture.

A possible existence of the heavier partner of $X(3872)$ with a similar value for the binding energy and mass $M = 4015$ MeV was first predicted in [13]. Then, such a state with $D^*\bar{D}^*$ molecular structure has been guessed as a consequence of the heavy-quark spin symmetry for the system under consideration in [14]. Later, the existence of an isoscalar 2^{++} $D^*\bar{D}^*$ partner of the $X(3872)$ has been predicted in a number of investigations using various phenomenological models (e.g., in Refs. [14–21]).

Recently, from the experimental side, the Belle collaboration has reported a hint of an isoscalar structure with mass $M = (4014.3 \pm 4.0 \pm 1.5)$ MeV and width $\Gamma = (4 \pm 11 \pm 6)$ MeV, seen in the $\gamma\psi(2S)$ invariant mass distribution via a two-photon process [22].

This new structure is located near the $D^*\bar{D}^*$ threshold, so one may conclude that it is a promising candidate for the corresponding loosely bound state. In particular, this structure was assumed to be a $D^*\bar{D}^*$ molecule with $J^{PC} = 0^{++}$ in [23, 24]. Furthermore, its measured width has the same order of magnitude as the prediction in [25, 26]. Nowadays, this narrow state is indeed a potential candidate for a ($D^*\bar{D}^*$) molecule with $J^{PC} = 2^{++}$.

Alternatively, within the conventional pattern of mesons, a 2^{++} tensor state with a similar mass could also be a conventional charmonium state in the first radial excitation $\chi_{c2}(3930)$ (see, e.g. Refs. [27, 28]).

Also, a compact tetraquark model has been employed to explore the 2^{++} states in [29–31].

In such a situation, the seemingly easiest way to disentangle these different multiquark configurations may be just to analyze the mass splitting between the 2^{++} and 1^{++} states. According to [14, 32], the corresponding mass splitting is approximately equal to that between the vector and pseudoscalar charmed mesons, that leads to a difference $\Delta M = M_{X_2(4014)} - M_{X(3872)} \approx 142$ MeV. However, the tetraquark approach predicted a much smaller difference

* ganbold@theor.jinr.ru

† ivanovm@theor.jinr.ru

$\Delta M \approx 80$ MeV [33]. For the difference between the charmonium $\chi_{c2}(3930)$ with 2^{++} and $X(3872)$ a similar conclusion has been found within the Godfrey-Isgur quark model [27] and a screened potential model [28] - but the corresponding differences ΔM are even less - about only 30 MeV and 40 MeV, respectively.

Another more complicated, but more reliable way to discriminate the various multiquark configurations of the spin-2 partner of the $X(3872)$ is to investigate the decay properties of the $X_2(4014)$ tensor state. In particular, a quark model in [34] provides estimates for the X_2 decay width to charmed mesons around tens of MeV by considering a 2^{++} tensor structure as the first radial excitation of the P -wave $\chi_{c2}(2^3P_2)$ charmonium. Then, the hadronic decays of the S -wave $D^*\bar{D}^*$ hadronic molecule, into $D\bar{D}$ and $D\bar{D}^*$ meson pairs were estimated to be small of the order of a few MeV [25] and, vice versa, as large as 50 MeV [26].

In a series of our previous papers we have studied some of the XYZ -states in the framework of the covariant confined quark model (CCQM) (for review, see e.g., [36, 37, 44]). The CCQM implements effective quark confinement realized by introducing an infrared cutoff of the proper time integration that prevents any singularities in matrix elements of the hadronic processes. In a number of papers, we have applied the CCQM to calculate the various physical observables like the form factors, angular decay characteristics, decay branchings etc. in the processes involving both light and heavy mesons and baryons. In particular, inspired by recent measurements we have studied the radiative decays of charmonium states below the $D\bar{D}$ threshold by introducing only one adjustable parameter common for the six charmonium states [35]. The obtained results were in good agreement with the latest data. We also predicted a narrower full width for the h_c charmonium than reported in PDG-2020.

We have treated the first exotic $X(3872)$ -meson as a diquark-antidiquark bound state and calculated its strong and electromagnetic decays in [38, 39]. The four-quark structure of the charged $Z_c(3900)$, $Z(4430)$, $X_b(5568)$, $Z_b(10610)$ and $Z'_b(10650)$ states has been examined by us in [40, 41]. The widths of the strong two-body decays $Z_c^+ \rightarrow J/\psi\pi^+$, $(\bar{D}^{(*)}D)$ and many others have also been calculated. It was found that the tetraquark-type current widely used in the literature for the $Z_c(3900)$ leads to a significant suppression of the $\bar{D}D^*$ and \bar{D}^*D modes. Contrary to this a molecular-type current provides an enhancement by a factor of 6-7 for the $\bar{D}D^*$ modes compared with the $Z_c^+ \rightarrow J/\psi\pi^+$, $\eta_c\rho^+$ modes, which is in agreement with experimental data from the BESIII Collaboration.

The $Y(4230)$ resonance has been analyzed in [43] as a four-quark state. Two options for the interpolating currents have been studied by using either the molecular-type current or tetraquark one. In both cases the widths of two-body decays $Y(4260) \rightarrow Z_c(3900) + \pi$ and $Y(4260) \rightarrow D^{(*)} + \bar{D}^{(*)}$ have been calculated. It was found that in both approaches the mode $Y \rightarrow Z_c^+ + \pi^-$ is enhanced compared with the open charm modes. More recently, strong decays of the charmonium-like state $Y(4320)$ have been studied within the CCQM. The resonance Y has been interpreted as a four-quark state with molecular-type interpolating current. We evaluated the hidden-charm decay width of Y into a vector and a scalar, with the latter decaying subsequently to a pair of charged pseudoscalar states. The strong decay mode $Y \rightarrow \pi^+\pi^-J/\Psi$ has been studied by involving the scalar resonances $f_0(500)$ and $f_0(980)$, considered quark-antiquark states, while the mode $Y \rightarrow K^+K^-J/\Psi$ - via $f_0(980)$. We have calculated the partial widths of the related strong decays and the branching ratio $\mathcal{B}(Y \rightarrow K^+K^-J/\Psi)/\mathcal{B}(Y \rightarrow \pi^+\pi^-J/\Psi)$, recently determined by the BESIII collaboration. The estimated branching ratio and calculated partial strong decay widths were in reasonable agreement with the latest experimental data [44].

In the light of these our findings, we below consider the $X_2(4014)$ state as a four-quark state of the molecular-type. We investigate the strong two-body decays $X_2 \rightarrow \omega J/\Psi$ and $X_2 \rightarrow \rho^0 J/\Psi$ in the framework of the CCQM.

The paper is organized as follows. A brief introduction to the CCQM and the general formalism for describing $X_2(4014)$ as four-quark state with molecular-type current are given in Section II. In Section III we determine the amplitudes and partial widths of the two-body strong decays $X_2 \rightarrow \omega J/\Psi$ and $X_2 \rightarrow \rho^0 J/\Psi$. We discuss the obtained results of calculation and compare them with latest theoretical predictions in Section IV. Our findings are summarized in Section V.

II Approach

The CCQM [45] represents an effective quantum field approach to hadronic physics and it is based on a relativistic Lagrangian describing the interaction of a hadron with its constituent quarks. It is a universal, pure relativistic, and a manifestly Lorentz covariant approach and allows one to study bound states with an arbitrary number of constituents and with arbitrary quantum numbers (spin-parity, isospin, flavor content, etc.) [46, 48–52]. Therefore, this model may serve an appropriate theoretical framework to analyze the strong decays of the exotic $X_2(4014)$ state.

According to the CCQM, a hadron described by a field $H(x)$ is coupled to a non-local quark current J_H carrying the hadron quantum numbers by the interaction Lagrangian.

In particular, the effective interaction Lagrangian, describing the coupling of the exotic state $H = X_2(4014)$, to its

constituent four quarks may be written in the form:

$$\mathcal{L}_{\text{int}} = g_H H_{\mu\nu}(x) \cdot J_H^{\mu\nu}(x) + \text{H.c.}, \quad (1)$$

where g_H is the renormalization coupling of the hadron H .

The interpolating four-quark molecular-type current for the neutral state $X_2(4014)$ with the quantum numbers $I^G(J^{PC}) = 0^+(2^{++})$ may be introduced as follows:

$$J_H^{\mu\nu} = \frac{1}{\sqrt{2}} \{ (\bar{q}\gamma^\mu c)(\bar{c}\gamma^\nu q) + (\gamma^\mu \leftrightarrow \gamma^\nu) \}. \quad (2)$$

The corresponding nonlocal generalization of the four-quark current within the CCQM reads

$$J_H^{\mu\nu}(x) = \int dx_1 \dots \int dx_4 \delta\left(x - \sum_{i=1}^4 w_i x_i\right) \Phi_H\left(\sum_{i<j} (x_i - x_j)^2\right) J_{H_{non}}^{\mu\nu}(x_1, \dots, x_4), \quad (3)$$

$$J_{H_{non}}^{\mu\nu} = \frac{1}{\sqrt{2}} \left\{ (\bar{q}(x_3)\gamma^\mu c(x_1)) \cdot (\bar{c}(x_2)\gamma^\nu q(x_4)) + (\gamma^\mu \leftrightarrow \gamma^\nu) \right\}, \quad (q = u, d),$$

where the reduced quark masses $w_i = m_i / \left(\sum_{j=1}^4 m_j\right)$ are specified for $m_1 = m_2 = m_c$ and $m_3 = m_4 = m_q$. Hereby, we neglect the isospin violation in the $u-d$ sector, i.e. $m_u = m_d = m_q$. The numbering of the coordinates x_i is chosen such that one has a convenient arrangement of vertices and propagators in the Feynman diagrams to be calculated.

The translationally invariant four-quark non-local vertex function Φ_H in Eq. (3) characterizes the quark distribution inside the hadron and reads:

$$\Phi_H\left(\sum_{i<j} (x_i - x_j)^2\right) = \prod_{i=1}^3 \int \frac{d^4 q_i}{(2\pi)^4} \tilde{\Phi}_H(-Q^2) e^{-iq_i(x_i - x_4)}, \quad Q^2 \doteq \frac{1}{2} \sum_{i \leq j} q_i q_j. \quad (4)$$

The Fourier transform of the translational invariant vertex function in momentum space is required to fall off in the Euclidean region in order to provide the ultraviolet convergence of the loop integrals. The vertex function $\tilde{\Phi}_H(-Q^2)$ is unique for the given hadron H and each hadron has its own adjustable parameter Λ_H , which can be related to the hadron 'size'. For most cases a pattern can be traced - the heavier a hadron, the larger its 'size'.

Below we use a simple Gaussian form as follows:

$$\tilde{\Phi}_H(-Q^2) = \exp(Q^2/\Lambda_H^2). \quad (5)$$

In fact, any choice for $\tilde{\Phi}_H$ is appropriate as long as it falls off sufficiently fast in the ultraviolet region to render the corresponding Feynman diagrams ultraviolet finite.

According to the CCQM, the renormalization coupling g_H of a hadron in Eq. (1) should be determined according to the so-called 'compositeness condition' [53, 54] which imposes that the renormalization constant of the hadron wave function has to be equal to zero as follows:

$$Z_H = 1 - g_H^2 \frac{d}{dp^2} \tilde{\Pi}_H(p^2) = 0, \quad p^2 = M_H^2, \quad (6)$$

where M_H is the hadron mass and $\tilde{\Pi}_H(p^2)$ is the diagonal (scalar) part of the hadron self-energy. The requirement $Z_H = 0$ implies that the physical state does not contain the bare state and is appropriately described as a bound state. The interaction leads to a dressed physical particle, i.e. its mass and wave function have to be renormalized. The condition $Z_H = 0$ also excludes effectively the constituent degrees of freedom from the space of physical states. It thereby guarantees the absence of double counting for the physical observable under consideration, the constituents only exist in virtual states.

In particular, the mass operator for the four-quark molecularly structured exotic state $X_2(4014)$ depicted in Fig. 1 reads

$$\begin{aligned} \tilde{\Pi}_{X_2}^{\mu\nu\rho\sigma}(p) = & \frac{N_c^2}{2} \prod_{i=1}^3 \int \frac{d^4 k_i}{(2\pi)^{4i}} \tilde{\Phi}_{X_2}^2(-(k_1^2 + k_2^2 + k_3^2 - k_1 k_2 - k_1 k_3 + k_2 k_3)/2) \\ & \times \left\{ \text{tr}[S_3(\not{k}_3 + w_3 \not{p})\gamma^\mu S_1(\not{k}_1 - w_1 \not{p})\gamma^\rho] \right. \\ & \times \text{tr}[S_2(\not{k}_2 + w_2 \not{p})\gamma^\nu S_4(-\not{k}_1 + \not{k}_2 + \not{k}_3 - w_4 \not{p})\gamma^\sigma] \\ & + \text{tr}[S_3(\not{k}_3 + w_3 \not{p})\gamma^\mu S_1(\not{k}_1 - w_1 \not{p})\gamma^\sigma] \\ & \left. \times \text{tr}[S_2(\not{k}_2 + w_2 \not{p})\gamma^\nu S_4(-\not{k}_1 + \not{k}_2 + \not{k}_3 - w_4 \not{p})\gamma^\rho] \right\}, \quad N_c = 3. \end{aligned} \quad (7)$$

The corresponding diagonal (scalar) part is defined as follows:

$$\tilde{\Pi}_{X_2}(p^2) = \frac{1}{5} \left(\frac{1}{2} \bar{g}_{\mu\rho} \bar{g}_{\nu\sigma} + \frac{1}{2} \bar{g}_{\mu\sigma} \bar{g}_{\nu\rho} - \frac{1}{3} \bar{g}_{\mu\nu} \bar{g}_{\rho\sigma} \right) \tilde{\Pi}_{X_2}^{\mu\nu\rho\sigma}(p), \quad \bar{g}_{\mu\nu} \doteq -g_{\mu\nu} + \frac{p_\mu p_\nu}{p^2}. \quad (8)$$

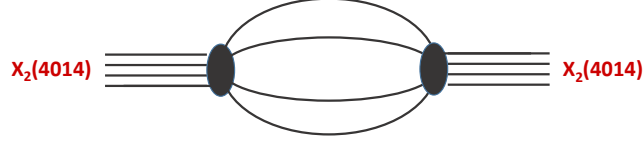


FIG. 1. Feynman diagram for the $X_2(4014)$ mass operator.

For the quark propagator we use the Fock-Schwinger representation:

$$\tilde{S}_j(k) = (m_j + \not{k}) \int_0^\infty d\alpha \exp(-\alpha(m_j^2 - k^2)). \quad (9)$$

Further on, we consider the hadron mass operator, matrix elements of hadronic decays and transitions, which are represented by quark-loop diagrams, which are described as convolutions of the corresponding quark propagators and vertex functions.

Then, the integration over quark-loop momenta can be performed for arbitrary Feynman diagram with n -quark propagators. The final result will be the multidimensional integration over the Fock-Schwinger parameters. Such integral contains all information on the analytical structure of the Feynman diagram including the branch points corresponding to the threshold singularities. These singularities lead to the imaginary part of the diagram if the ingoing energy larger than sum of quark masses. Physically this means that the quarks may appear in the observed spectrum.

In order to solve the quark confinement problem the following trick has been used. First, one has to transform the integral over an infinite space of the Fock-Schwinger parameters into an integral over a simplex convoluted with only one-dimensional improper integral. One has

$$\begin{aligned} \Pi &= \int_0^\infty d^n \alpha W(\alpha_1, \dots, \alpha_n) = \int_0^\infty d^n \alpha \underbrace{\int_0^\infty dt \delta\left(t - \sum_{i=1}^n \alpha_i\right)}_{=1} W(\alpha_1, \dots, \alpha_n) \\ &= \int_0^\infty dt t^{n-1} \int_0^\infty d^n \alpha \delta\left(1 - \sum_{i=1}^n \alpha_i\right) W(t\alpha_1, \dots, t\alpha_n), \end{aligned} \quad (10)$$

where the integration over dimensionless α_i parameters proceeds over a simplex. Now there is the only dimensional parameter "t" which is nothing as the Fock proper time.

The cut-off parameter λ is then introduced in a natural way as follows:

$$\int_0^\infty dt t^{n-1} \dots \rightarrow \int_0^{1/\lambda^2} dt t^{n-1} \dots \quad (11)$$

Such a cut-off makes the integral to be an analytic function without any singularities. In this way all potential thresholds in the quark-loop diagrams are removed together with corresponding branch points [45]. Within the CCQM, the cut-off parameter is universal for all processes and its value, as obtained from a fit to data, equals to

$$\lambda_{\text{cut-off}} = 0.181 \text{ GeV}. \quad (12)$$

The resulting integrals are computed numerically.

The CCQM consists of several basic parameters: the universal infrared cutoff parameter λ , the constituent quark masses m_q and the hadron 'size' parameters Λ_H . For given value of the size parameter Λ_H the coupling constant g_H of hadron H is strictly fixed by the requirements of Eq. (6) and do not constitute further free parameters. The model parameters are determined by minimizing χ^2 in a fit to the latest available experimental data and some lattice results. In doing so, we have observed that the errors of the fitted parameters are of the order of $\sim 10\%$. The central values of the basic parameters updated in Refs. [47, 50] are shown in Table I. Obviously, the errors of our calculations within the CCQM are expected to be about $\pm 10\%$.

Below we apply the CCQM to estimate the strong decays of the spin-2 partner $X_2(4014)$ of the charmonium-like state $X(3872)$.

III Strong decays of $X_2(4014)$ into $\omega J/\psi$ and $\rho^0 J/\psi$

The ratio of the branching fractions

$$\text{BR}_{X_2} \doteq \frac{\Gamma(X_2 \rightarrow \omega J/\psi)}{\Gamma(X_2 \rightarrow \rho^0 J/\psi)} \quad (13)$$

has recently been investigated using the effective Lagrangian approach by assuming the X_2 as a molecular state of $D^* \bar{D}^*$ [55]. The only contributions from the triangle hadron loops made of the charmed mesons D^* and \bar{D}^* have been considered.

It has been found that the decay widths are quite sensitive to the X_2 mass. At the present center mass $M_{X_2} = 4.0143 \text{ GeV}$, the width for the $X_2 \rightarrow J/\psi \rho^0$ was a few tens of keV, while it is on the order of $10^2 - 10^3 \text{ keV}$ for the $X_2 \rightarrow J/\psi \omega$. The corresponding width ratio was calculated to be

$$\text{BR}_{X_2} \approx 15, \quad (14)$$

i.e. one order of magnitude larger than that for the case of $X(3872)$ which approaches unity.

Below, we consider the $X_2(4014)$ as a four-quark state with a molecular-type interpolating current and study its strong decays into $\omega J/\psi$ and $\rho^0 J/\psi$ in the framework of the CCQM [45]. In doing so, we limit ourselves by considering only the LO contributions corresponding to the two-petal quark loops represented by the Feynman diagram in Fig. 2. We calculate the partial widths of the related strong decays and estimate the branching ratio mentioned in Eq. (13).

We note that the description of the $c\bar{c} - q\bar{q}$ transitions, which go via gluon exchange, is out of the CCQM scope.

The invariant matrix element for the strong decay $X_2 \rightarrow J/\psi + V$ reads

$$\mathcal{M}_{X_2 JV} \equiv i (2\pi)^4 \delta^{(4)}(p - p_1 - p_2) \varepsilon_{\mu\nu}(p) \varepsilon_\rho^*(p_1) \varepsilon_\sigma^*(p_2) T_{X_2 JV}^{\mu\nu\rho\sigma}(p_1, p_2), \quad (15)$$

where $\{p, p_1, p_2\}$ and $\varepsilon_{\mu\nu}(p)$, $\varepsilon_\rho^*(p_1)$, $\varepsilon_\sigma^*(p_2)$ are the momenta and polarization vectors of the X_2 , J/ψ and the vector meson $V = \{\omega, \rho^0\}$, correspondingly.

The polarization vectors of the tensor and vector mesons satisfy the symmetry, transversality, tracelessness, orthonormality and completeness conditions as follows:

$$\begin{aligned} \varepsilon_{\mu\nu}^{(\lambda)}(p) &= \varepsilon_{\nu\mu}^{(\lambda)}(p), \quad \varepsilon_{\mu\nu}^{(\lambda)}(p) p^\mu = 0, \quad \varepsilon_{\mu\nu}^{(\lambda)}(p) g^{\mu\nu} = 0, \quad \varepsilon_{\mu\nu}^{\dagger(\lambda)} \varepsilon^{(\lambda')\mu\nu} = \delta_{\lambda\lambda'}, \\ \tilde{g}_{\mu\nu\alpha\beta} &\doteq \sum_{\lambda=0,\pm 1,\pm 2} \varepsilon_{\mu\nu}^{(\lambda)} \varepsilon_{\alpha\beta}^{\dagger(\lambda)} = \frac{1}{2} (\bar{g}_{\mu\alpha} \bar{g}_{\nu\beta} + \bar{g}_{\mu\beta} \bar{g}_{\nu\alpha}) - \frac{1}{3} \bar{g}_{\mu\nu} \bar{g}_{\alpha\beta}, \quad \bar{g}_{\mu\nu} \doteq -g_{\mu\nu} + \frac{p_\mu p_\nu}{p^2}, \\ \epsilon_\mu^{(\lambda)}(p) p^\mu &= 0, \quad \sum_{\lambda=0,\pm} \epsilon_\mu^{(\lambda)}(p) \epsilon_\nu^{\dagger(\lambda)}(p) = \bar{g}_{\mu\nu}, \quad \epsilon_\mu^{\dagger(\lambda)} \epsilon^{(\lambda')\mu} = -\delta_{\lambda\lambda'}. \end{aligned} \quad (16)$$

In the leading order, the decay amplitude in Eq. (15) reads

$$\begin{aligned} T_{X_2 JV}^{\mu\nu\rho\sigma}(p_1, p_2) &= g_{X_2} g_{J/\psi} g_V \\ &\times \frac{N_c^2}{2} \int \frac{d^4 k_1}{(2\pi)^4 i} \int \frac{d^4 k_2}{(2\pi)^4 i} \tilde{\Phi}_{X_2}(-Q^2) \tilde{\Phi}_{J/\psi}(-(\ell_1 + \ell_2)^2/4) \tilde{\Phi}_V(-(\ell_3 + \ell_4)^2/4) \\ &\times \left\{ \text{tr} [\gamma^\mu S_1(\ell_1) \gamma^\rho S_2(\ell_2) \gamma^\nu S_4(\ell_4) \gamma^\sigma S_3(\ell_3)] + \text{tr} [\gamma^\nu S_1(\ell_1) \gamma^\rho S_2(\ell_2) \gamma^\mu S_4(\ell_4) \gamma^\sigma S_3(\ell_3)] \right\}, \end{aligned} \quad (17)$$

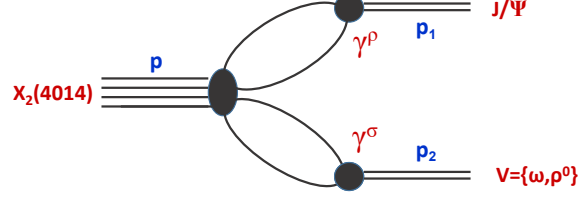


FIG. 2. Feynman diagram describing the decay $X \rightarrow J/\psi + V$, here $V = \{\omega, \rho^0\}$.

with the following notations introduced:

$$\begin{aligned}\tilde{\Phi}_H(-k^2) &= \exp(k^2/\Lambda_H^2), \quad H = \{X_2, J/\psi, V\}, \\ Q^2 &= [(\ell_1 + pw_1)^2 + (\ell_2 - pw_2)^2 + (\ell_3 + pw_3)^2 + (\ell_4 - pw_4)^2] / 2, \\ \ell_1 &= k_1 - pw_1, \quad \ell_2 = k_1 - pw_1 - p_1, \quad \ell_3 = k_2 - pw_4 - p_2, \quad \ell_4 = k_2 - pw_4.\end{aligned}$$

As mentioned above, the renormalized couplings g_{X_2} , $g_{J/\psi}$ and g_V are strictly determined by the self-energy (mass) function of the corresponding hadrons, (see Eq. (6)).

By substituting the corresponding Gaussian-type vertices functions and the quark propagators in Eq. (17), and performing an explicit $k_{1,2}$ -integrations while turning the set of Fock-Schwinger parameters into a simplex, we obtain the LO amplitude of the strong decay $X_2 \rightarrow J/\psi + V$ as follows:

$$\begin{aligned}T_{X_2 JV}^{\mu\nu\rho\sigma}(p_1, p_2) &= A_V \cdot \left(g^{\mu\rho} [g^{\sigma\nu}(p_1 \cdot p_2) - p_1^\sigma p_2^\nu] + g^{\nu\rho} [g^{\sigma\mu}(p_1 \cdot p_2) - p_1^\sigma p_2^\mu] \right) \\ &+ B_V \cdot \left(g^{\sigma\rho} [p_1^\mu p_2^\nu + p_1^\nu p_2^\mu] - g^{\mu\sigma} p_1^\nu p_2^\rho - g^{\nu\sigma} p_1^\mu p_2^\rho \right),\end{aligned}\quad (18)$$

where the two independent form factors $A_V(g_X, g_{J/\psi}, g_V, p^2, p_1^2, p_2^2)$ and $B_V(g_X, g_{J/\psi}, g_V, p^2, p_1^2, p_2^2)$ are determined according to Eq. (17).

Consequently, we calculate

$$|\mathcal{M}_{X_2 JV}|^2 \sim |\varepsilon_{\mu\nu}(p) \varepsilon_\rho^*(p_1) \varepsilon_\nu^*(p_2) T_{X_2 JV}^{\mu\nu\rho\sigma}|^2 = M_{X_2}^4 (C_A^V \cdot A_V^2 + C_{AB}^V \cdot A_V \cdot B_V + C_B^V \cdot B_V^2), \quad (19)$$

where the coefficients C_A^V , C_{AB}^V and C_B^V are completely defined through the meson masses as follows:

$$\begin{aligned}C_A^V &\doteq [(3 + 2\xi_V) \xi_J^4 + (1 - \xi_V)^4 (3 + 2\xi_V) + (28 + 20\xi_V - 8\xi_V^2) \xi_J^3 \\ &+ 4\xi_J(1 - \xi_V)^2(7 + 5\xi_V - 2\xi_V^2) - 2\xi_J^2(31 - 52\xi_V + 27\xi_V^2 - 6\xi_V^3)] / (12\xi_J), \\ C_{AB}^V &\doteq [\xi_J^4(7 - 2\xi_V) - (1 - \xi_V)^4(3 + 2\xi_V) - 2\xi_J^3(9 + 5\xi_V - 4\xi_V^2) \\ &+ 2\xi_J(1 - \xi_V)^2(1 + 5\xi_V + 4\xi_V^2) + 4\xi_J^2(3 - \xi_V + \xi_V^2 - 3\xi_V^3)] / (6\xi_J), \\ C_B^V &\doteq [3 + 4\xi_J + 2\xi_V](\xi_J^2 + (1 - \xi_V)^2 - 2\xi_J(1 + \xi_V))^2 / (12\xi_J),\end{aligned}\quad (20)$$

where $\xi_J \doteq M_{J/\psi}^2/M_{X_2}^2$ and $\xi_V \doteq M_V^2/M_{X_2}^2$ for $V = \{\rho^0, \omega\}$.

The two-body strong decay width reads:

$$\Gamma_{X_2 JV} = \frac{1}{2S+1} \frac{|\vec{p}_2|}{8\pi M_{X_2}^2} \sum_{polar} |\mathcal{M}_{X_2 JV}|^2, \quad (21)$$

where $|\vec{p}_2| \doteq \lambda^{1/2}(M_{X_2}^2, M_{J/\psi}^2, M_V^2)/(2M_{X_2})$ and $\lambda(x, y, z) \doteq x^2 + y^2 + z^2 - 2(xy + xz + yz)$ is the Källén kinematical function while $S = 2$ is the spin value of X_2 .

IV Numerical Results

Many experimental and theoretical investigations are devoted to understand the nature of the exotic XYZ family and considerable results have been achieved to determine the mass, width, and main quantum numbers (for reviews see, e.g. [56, 57, 60]).

In particular, a recent observation of a structure in the invariant mass distribution of the $\gamma\psi(2S)$ with a mass of $4014.3 \pm 4.0 \pm 1.5$ MeV and a width of $4 \pm 11 \pm 6$ MeV by the Belle collaboration [58] has become a stimulating motive in the investigation of the exotic XYZ states despite a low global significance of 2.8σ of the new structure.

In this Section, we systematically continue our investigation of the hidden charmonium decays of the exotic XYZ states and consider the two-body strong decays of the spin-2 partner of $X(3872)$, namely $X_2 \rightarrow \rho^0 J/\psi$ and $X_2 \rightarrow \omega J/\psi$. We assume a four-quark content of X_2 with a pure $D^*\bar{D}^*$ mesonic molecule structure. In doing so, we consider only the LO contributions to the decays corresponding to the two-leaf Feynman diagram shown in Fig. 2 in the framework of the CCQM approach.

The model parameters in the CCQM are determined by minimizing χ^2 in fits to the latest available experimental data and some lattice results. The fitted parameters may vary around their central value by about few percents, and the errors of our calculations do not exceed $\pm 10\%$ percents.

The most of hadron 'size' parameters in the CCQM are more or less rigidly fixed by fitting to available experimental data (see, e.g. in [35, 43]). The updated central values of the basic CCQM parameters, namely, the universal infrared cutoff parameter λ , the constituent quark masses ($m_{u/d}, m_c$) and the hadron 'size' parameters (Λ_H) are partly shown in Table I. We proceed with our computations using these values, which remain unaltered.

TABLE I. Model basic parameter values (in GeV).

λ	$m_{u/d}$	m_c	Λ_{ρ^0}	Λ_ω	$\Lambda_{J/\psi}$
0.181	0.241	1.670	0.61	0.80	1.55

First, we calculate the renormalized couplings g_H of the participating mesons ($H = \{J/\psi, \omega, \rho^0\}$) according to Eq. (6). The numerical values of g_H estimated in dependence on the 'size' parameters Λ_H are given in Fig. 3.

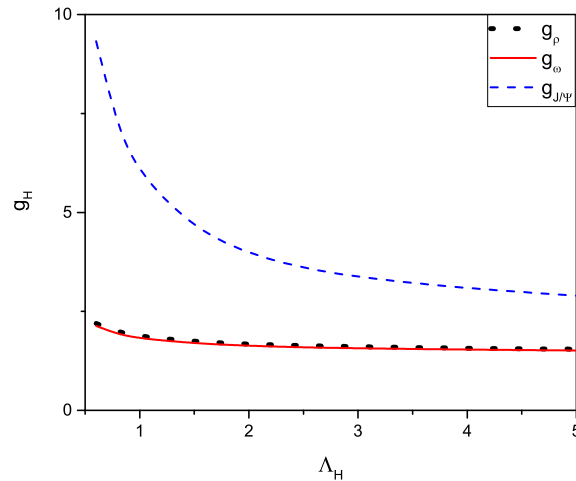


FIG. 3. The renormalized couplings g_H of the mesons ($H = \{\rho^0, \omega, J/\psi\}$) calculated in dependence on the 'size' parameters Λ_H (in GeV).

We change the only totally adjustable size parameter Λ_{X_2} at the appropriate intervals for the numerical evaluation of the strong decay widths of X_2 .

Remember, we utilized the 'size' parameter value of the tetraquark state $X(3872)$ in the interval $\Lambda_X \in [3.0 \div 4.0]$ GeV in our previous study [59]. More recently, the 'size' value for a heavier exotic state $Y(4230)$ has been corrected to $\Lambda_Y \in [5.15 \pm 0.26]$ GeV in [44].

Because the physical mass of the X_2 state is between two masses, $M_X = 3.872$ GeV and $M_Y = 4.222$ GeV, we will search for the necessary parameter Λ_{X_2} in the range of (3.5 - 5.5) GeV by adhering to the model's pattern - 'the heavier a hadron, the larger its size'.

Then, using Eq. (21), we can estimate the hidden charm partial decay widths of the two-body strong decays of X_2 , once the renormalization couplings g_H have been computed.

1. Let us first make a simple and rough approximation to the desired branching ratio BR_{X_2} . We easily calculate the ratios between the relevant phase spaces and corresponding renormalized couplings as follows:

$$\frac{\lambda^{1/2}(M_{X_2}^2, M_{J/\psi}^2, M_\omega^2)}{\lambda^{1/2}(M_{X_2}^2, M_{J/\psi}^2, M_{\rho^0}^2)} \approx 0.976, \quad \frac{g_\omega^2}{g_{\rho^0}^2} \approx 0.780. \quad (22)$$

Then, by neglecting the difference between the corresponding form factors C_*^ω and $C_*^{\rho^0}$ ($*$ = {A, AB, B}) defined in Eq. (20), one can approximately write down the ratio:

$$\text{BR}_{X_2}^{\text{approx}} \approx 0.762 \quad (23)$$

that is less than unity.

2. Now we take into account accurately the real contributions of the matrix elements and calculate the partial decay widths defined in Eq. (21) in dependence on the 'size' parameter Λ_{X_2} . The obtained results are represented in Fig. 4 for a fixed central value of the exotic state mass $M_{X_2} = 4.014$ GeV.

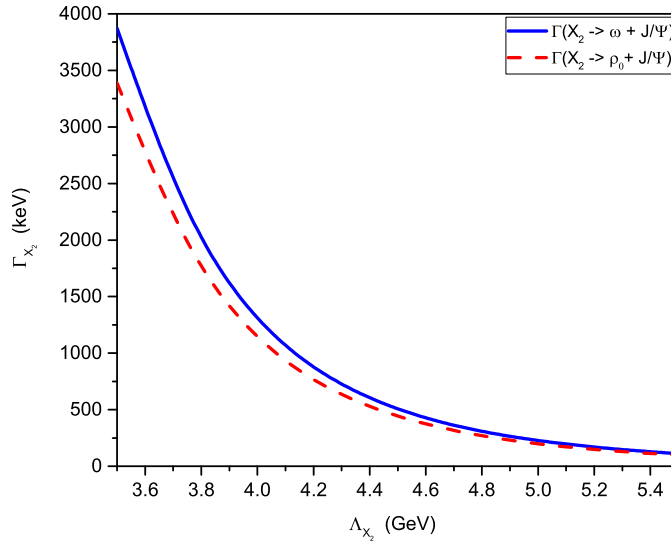


FIG. 4. The dependencies of the partial decay widths $\Gamma(X_2 \rightarrow \omega J/\psi)$ and $\Gamma(X_2 \rightarrow \rho^0 J/\psi)$ on the 'size' parameter Λ_{X_2} for a fixed central value of the exotic state mass $M_{X_2} = 4.014$ GeV.

One can see in Fig. 4 that both the partial decay widths decrease monotonically as the 'size' parameter Λ_{X_2} increases.

i) Accordingly, if we admit that the partial two-body strong decay widths $\Gamma(X_2 \rightarrow \omega J/\psi)$ and $\Gamma(X_2 \rightarrow \rho^0 J/\psi)$ are of hundreds keV , then our estimates impose a certain restriction on the allowed 'size' parameter within an interval $\Lambda_{X_2} \in [4.0 \div 5.5]$ GeV.

ii) However, the corresponding ratio of these partial widths

$$\text{BR}_{X_2}^{\text{CCQM}} \doteq \frac{\Gamma(X_2 \rightarrow \omega J/\psi)}{\Gamma(X_2 \rightarrow \rho^0 J/\psi)} = 1.143 \sim 1.147 \quad \text{for} \quad \Lambda_{X_2} \in [3.5, 5.5] \text{ GeV} \quad (24)$$

almost cancels or at least weakens the 'size'-dependence.

3. Recently, by assuming the X_2 as a pure molecule of the $D^*\bar{D}^*$, the hidden charmonium decays of the $X_2 \rightarrow \omega J/\psi$ and $X_2 \rightarrow \rho^0 J/\psi$ via the intermediate meson loops have been estimated in a framework of the effective field theory [55].

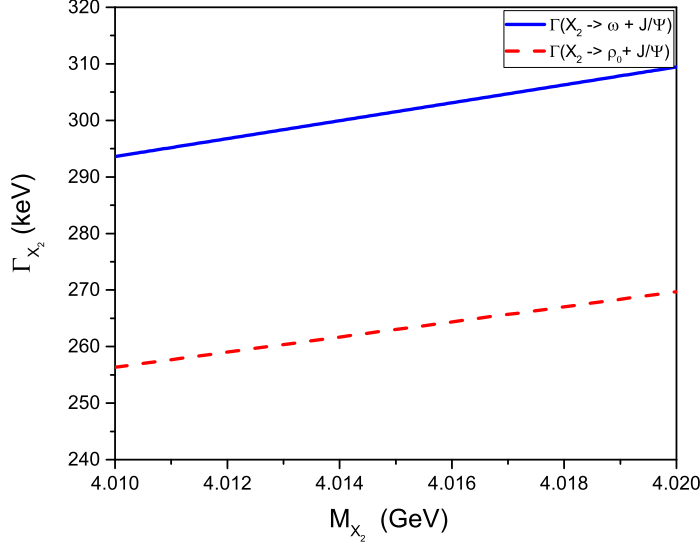


FIG. 5. The dependencies of the partial decay widths $\Gamma(X_2 \rightarrow \omega J/\psi)$ and $\Gamma(X_2 \rightarrow \rho^0 J/\psi)$ on the exotic state mass M_{X_2} for a fixed 'size' parameter value $\Lambda_{X_2} = 4.80$ GeV.

The results indicated that the decay widths are strongly dependent on the X_2 mass. In particular, within a short interval for the mass of X_2 ranging from 4.009 GeV to 4.020 GeV, the width ranges from ~ 0.2 to 200 keV for $X_2 \rightarrow \rho^0 J/\psi$, while for $X_2 \rightarrow \omega J/\psi$ it is between 0.1 and 1.5 MeV. Hereby, the width for $X_2 \rightarrow \rho^0 J/\psi$ first increases with the X_2 mass to a peak value at $m_{X_2} = 4.0137$ GeV, then drops until ~ 4.0167 GeV, and finally starts to increase again. However, the width for $X_2 \rightarrow \omega J/\psi$ shows opposite variations with the X_2 mass at a given α , i.e., the width exhibits a valley at $m_{X_2} = 4.0137$ GeV, while near $m_{X_2} = 4.0175$ GeV it is a peak. At present center value of the mass 4014.3 MeV, the width for the $X_2 \rightarrow \rho^0 J/\psi$ is predicted to be a few tens of keV, while it is on the order of 10^{2-3} keV for the $X_2 \rightarrow \omega J/\psi$ [55].

We have also investigated the dependence of the partial decay widths $\Gamma(X_2 \rightarrow \omega J/\psi)$ and $\Gamma(X_2 \rightarrow \rho^0 J/\psi)$ on the exotic hadron mass deviation within the experimental uncertainty reported in [22]. The corresponding numerical results are shown in Fig. 5 for a given value of 'size' parameter $\Lambda_{X_2} = 4.80$ GeV.

Our numerical results indicate that the decay widths slowly increase without any peaks and drops. In the mass interval from 4.010 GeV to 4.020 GeV, the decay width ranges from 294 to 309 keV for $X_2 \rightarrow \omega J/\psi$, while for $X_2 \rightarrow \rho^0 J/\psi$ it is between 257 and 270 keV, by keeping the branching ratio constant $\text{BR}_{X_2}^{\text{CCQM}} = 1.14$.

This result is not surprisingly. The hidden charm decays of the X_2 in our approach occur via the confined quark loops but not the charmed D^* and \bar{D}^* meson loops, without any threshold effects.

V Summary

The hidden-charm strong decays of the spin-2 exotic charmonium-like state $X_2(4014)$ into channels $\omega J/\Psi$ and $\rho^0 J/\Psi$ have been studied within the framework of the covariant confined quark model, designed to eliminate any UV divergences in quark loops.

We have interpreted the exotic hadron X_2 as a four-quark state with a $D^*\bar{D}^*$ molecular-type interpolating quark current and computed the leading-order strong decay widths at the level of two-petal quark-loop diagrams.

We have calculated the partial widths of the above-mentioned decay modes and their branching ratio recently discussed in literature [21, 55]. In our calculation, we used the average mass and full decay width of the X_2 state

reported by the Belle Collaboration [22].

Our findings are:

i. The partial strong-decay widths $\Gamma(X_2 \rightarrow \omega J/\psi)$ and $\Gamma(X_2 \rightarrow \rho^0 J/\psi)$ depend significantly on the model size parameter Λ_{X_2} , decreasing rapidly from 3 - 4 MeV to several hundreds of keV in the reasonable interval (3.5 - 5.5 GeV) for a fixed mass $M_{X_2} = 4.014$ GeV.

ii. We may calculate a simple and rough approximation of the corresponding branching ratio by taking into account only effects due to the phase space factors and renormalized couplings as follows: $\text{BR}_{X_2}^{\text{approx}} \approx 0.762$.

However, our accurate numerical results represented in Fig. 5 clearly show that the ratio $\text{BR}_{X_2}^{\text{CCQM}} \simeq 1.14$ is larger than unity and almost independent of Λ_{X_2} . This may indicate a relative dominance of the $\omega J/\psi$ decay mode.

iii. We have also investigated the sensibility of our numerical results on the exotic hadron mass deviation under the data uncertainty reported in [22]. Remember that the corresponding numerical results for the decay widths and the ratio reported in [21, 55] demonstrated very strong dependencies on the X_2 mass value.

Our numerical results show that the decay widths monotonically increase with no peaks and drops in the mass interval from 4.010 GeV to 4.020 GeV; the width ranges from 294 to 309 keV for $X_2 \rightarrow J/\psi\omega$, while for $X_2 \rightarrow J/\psi\rho^0$, it is between 257 and 270 keV, by keeping the branching ratio almost constant ($\text{BR}_{X_2}^{\text{CCQM}} = 1.14$).

The reason is simple: the hidden charm decays of the X_2 in our approach occur via the confined quark loops but not the charmed D^* and \bar{D}^* meson loops, so with no threshold effects.

By conclusion, the exotic spin-2 state X_2 has been interpreted as a four-quark state of molecular-type interpolating current within the CCQM. We have calculated the strong decay (to $\omega J/\psi$ and $\rho^0 J/\psi$) widths of the exotic state and estimated the corresponding branching ratio.

We have maintained the basic CCQM parameters in our calculation, adding only one new tunable size parameter (Λ_{X_2}) to represent the quark distribution inside the hadron.

Our numerical results show that the strong decay widths under consideration change smoothly, but their ratio $\text{BR}_{X_2}^{\text{CCQM}} = 1.14$ is almost constant in the wide and reasonable interval.

Our numerical results indicate that the strong decay widths under consideration vary smoothly, but within the wide and tolerable interval $\Lambda_{X_2} \in [3.5 - 5.5]$ GeV, their ratio is nearly constant ($\text{BR}_{X_2}^{\text{CCQM}} = 1.14$).

Additionally, it was discovered that the decay widths under investigation showed only a minor sensitivity to the mass variation of X_2 determined in the most recent experiment [22].

We draw the conclusion that the estimated branching ratio and hidden-charm strong-decay widths are in good accord with the most recent theoretical predictions in [21, 55] and may support the four-quark molecular-type structure of X_2 .

We anticipate that further, more accurate experimental data on the X_2 's particle characteristics will enable us to refine the model's parameters and make more intelligible deductions regarding the underlying workings of this exotic state.

-
- [1] Hua-Xing Chen, Wei Chen, Xiang Liu, and Shi-Lin Zhu, Phys. Rep. **639**, 1 (2016), [arXiv:1601.02092 [hep-ph]].
 - [2] A. Esposito, A. Pilloni, and A. D. Polosa, Phys. Rep. **668**, 1 (2017), [arXiv:1611.07920 [hep-ph]].
 - [3] Feng-Kun Guo, Christoph Hanhart, Ulf-G. Meissner, Qian Wang, Qiang Zhao, and Bing-Song Zou, Rev. Mod. Phys. **90**, 015004 (2018), [arXiv:1705.00141 [hep-ph]].
 - [4] Nora Brambilla, Simon Eidelman, Christoph Hanhart, Alexey Nefediev, Cheng-Ping Shen, Christopher E. Thomas, Antonio Vairo, and Chang-Zheng Yuan, Phys. Rep. **873**, 1 (2020), [arXiv:1907.07583 [hep-ex]].
 - [5] Hua-Xing Chen, Wei Chen, Xiang Liu, Yan-Rui Liu, and Shi-Lin Zhu, Rept. Prog. Phys. **86**, 026201 (2023), [arXiv:2204.02649 [hep-ph]].
 - [6] S.-K. Choi, S.L. Olsen *et al.* [Belle Collaboration], Phys. Rev. Lett. **91**, 262001 (2003), [arXiv:hep-ex/0309032].
 - [7] R. Aaij *et al.* [LHCb Collaboration], Phys. Rev. Lett. **110**, 222001 (2013).
 - [8] S. Fleming and T. Mehen, Phys. Rev. D **78**, 094019 (2008).
 - [9] Thomas Mehen, Phys. Rev. D **92**, 034019 (2015).
 - [10] Yu. S. Kalashnikova and A. V. Nefediev, Phys. Usp. **62**, 568 (2019).
 - [11] Lu Meng, Guang-Juan Wang, Bo Wang, and Shi-Lin Zhu, Phys. Rev. D **104**, 094003 (2021).
 - [12] an Wang, Qi Wu, Gang Li, Wen-Hua Qin, Xiao-Hai Liu, Chun-Sheng An, and Ju-Jun Xie, Phys. Rev. D **106**, 074015 (2022).
 - [13] Nils A. Tornqvist, Z. Phys. C **61**, 525 (1994).
 - [14] J. Nieves and M. Pavaon Valderrama, Phys. Rev. D **86**, 056004 (2012), [arXiv:1204.2790 [hep-ph]].
 - [15] R. Molina and E. Oset, Phys. Rev. D **80**, 114013 (2009), [arXiv:0907.3043 [hep-ph]].
 - [16] C.Hidalgo-Duque, J.Nieves, A. Ozpineci, and V. Zamiralov, Phys. Lett. B **727**, 432 (2013).

- [17] M. Albaladejo, F.-K. Guo, C. Hidalgo-Duque, J. Nieves, and M.P. Valderrama, *Eur. Phys. J. C* **75**, 547 (2015).
- [18] V. Baru, E. Epelbaum, A.A. Filin, C. Hanhart, U.-G. Meissner, and A.V. Nefediev, *Phys. Lett. B* **763**, 20 (2016).
- [19] Ortega, Pablo G. and Segovia, Jorge and Entem, David R. and Fernández, Francisco, *Phys. Lett. B* **778**, 1 (2018).
- [20] Dong, Xiang-Kun and Guo, Feng-Kun and Zou, Bing-Song, *Prog. Phys.* **41**, 65 (2021).
- [21] P.-P. Shi, J.M. Dias, and F.-K. Guo, *Phys. Lett. B* **843**, 137987 (2023).
- [22] X. L. Wang *et al.* [Belle Collaboration], *Phys. Rev. D* **105**, 112011 (2022).
- [23] Zi-Li Yue, Man-Yu Duan, Chun-Hua Liu, Dian-Yong Chen, and Yu-Bing Dong, *Phys. Rev. D* **106**, 054008 (2022), [arXiv:2208.12796 [hep-ph]].
- [24] Man-Yu Duan, Dian-Yong Chen, and En Wang, *Eur. Phys. J. C* **82**, 968 (2022), [arXiv:2207.03930 [hep-ph]].
- [25] M. Albaladejo, F.-K. Guo, C. Hidalgo-Duque, J. Nieves, and M. Pavon Valderrama, *Eur. Phys. J. C* **75**, 547 (2015), [arXiv:1504.00861 [hep-ph]].
- [26] V. Baru, E. Epelbaum, A. A. Filin, C. Hanhart, Ulf-G. Meissner, and A. V. Nefediev, *Phys. Lett. B* **763**, 20 (2016), [arXiv:1605.09649 [hep-ph]].
- [27] Stephen Godfrey and Nathan Isgur, *Phys. Rev. D*, **32** 189 (1985).
- [28] Bai-Qing Li, Ce Meng, and Kuang-Ta Chao, *Phys. Rev. D* **80**, 014012 (2009), [arXiv:0904.4068 [hep-ph]].
- [29] Jing Wu, Xiang Liu, Yan-Rui Liu, and Shi-Lin Zhu, *Phys. Rev. D* **99**, 014037 (2019), [arXiv:1810.06886 [hep-ph]].
- [30] Pan-Pan Shi, Fei Huang, and Wen-Ling Wang, *Phys. Rev. D* **103**, 094038 (2021), [arXiv:2105.02397 [hep-ph]].
- [31] Jesse F. Giron, Richard F. Lebed, and Steven R. Martinez, *Phys. Rev. D* **104**, 054001 (2021), [arXiv:2106.05883 [hep-ph]].
- [32] Feng-Kun Guo, Carlos Hidalgo-Duque, Juan Nieves, and Manuel Pavon Valderrama, *Phys. Rev. D* **88**, 054007 (2013), [arXiv:1303.6608 [hep-ph]].
- [33] L. Maiani, F. Piccinini, A. D. Polosa, and V. Riquer, *Phys. Rev. D* **89**, 114010 (2014), [arXiv:1405.1551 [hep-ph]].
- [34] T. Barnes, S. Godfrey, and E. S. Swanson, *Phys. Rev. D* **72**, 054026 (2005), [arXiv:hep-ph/0505002].
- [35] Gurjav Ganbold, Thomas Gutsche, Mikhail A. Ivanov, and Valery E. Lyubovitskij, *Phys. Rev. D* **104**, 094048 (2021), [arXiv:2107.08774 [hep-ph]].
- [36] M. Ivanov, EPJ Web Conf. **192**, 00042 (2018), [arXiv:1809.02973 [hep-ph]].
- [37] S. Dubnička, A. Z. Dubničková, M. A. Ivanov, and A. Liptaj, *Symmetry* **12**, no.6, 884 (2020).
- [38] S. Dubnička, A. Z. Dubničková, M. A. Ivanov, and J. G. Körner, *Phys. Rev. D* **81**, 114007 (2010), [arXiv:1004.1291 [hep-ph]].
- [39] S. Dubnička, A. Z. Dubničková, M. A. Ivanov, J. G. Körner, P. Santorelli and G. G. Saidullaeva, *Phys. Rev. D* **84**, 014006 (2011), [arXiv:1104.3974 [hep-ph]].
- [40] F. Goerke, T. Gutsche, M. A. Ivanov, J. G. Korner, V. E. Lyubovitskij, and P. Santorelli, *Phys. Rev. D* **94**, no.9, 094017 (2016), [arXiv:1608.04656 [hep-ph]].
- [41] F. Goerke, T. Gutsche, M. A. Ivanov, J. G. Körner and V. E. Lyubovitskij, *Phys. Rev. D* **96**, 054028 (2017), [arXiv:1707.00539 [hep-ph]].
- [42] T. Gutsche, M. A. Ivanov, J. G. Körner, V. E. Lyubovitskij, and K. Xu, *Phys. Rev. D* **96**, 114004 (2017), [arXiv:1710.02357 [hep-ph]].
- [43] S. Dubnička, A. Z. Dubničková, A. Issadykov, M. A. Ivanov, and A. Liptaj, *Phys. Rev. D* **101**, 094030 (2020), arXiv:2003.04142 [hep-ph].
- [44] Gurjav Ganbold and M.A.Ivanov, *Eur. Phys. J. A* **60**, 13 (2024), [arXiv:2303.09333 [hep-ph]].
- [45] T. Branz, A. Faessler, T. Gutsche, M. A. Ivanov, J. G. Körner, and V. E. Lyubovitskij, *Phys. Rev. D* **81**, 034010 (2010), [arXiv:0912.3710 [hep-ph]].
- [46] M. A. Ivanov, J. G. Körner, S. G. Kovalenko, P. Santorelli, and G. G. Saidullaeva, *Phys. Rev. D* **85**, 034004 (2012); T. Gutsche, M. A. Ivanov, J. G. Körner, V. E. Lyubovitskij, and P. Santorelli, *Phys. Rev. D* **86**, 074013 (2012); F. Goerke, T. Gutsche, M. A. Ivanov, J. G. Korner, V. E Lyubovitskij, and P. Santorelli, *Phys. Rev. D* **94**, 094017 (2016); M. A. Ivanov, J. G. Körner, and C. T. Tran, *Phys. Rev. D* **94**, 094028 (2016); T. Gutsche, M. A. Ivanov, J. G. Körner, V. E. Lyubovitskij, V. L. Lyubushkin, and P. Santorelli, *Phys. Rev. D* **96**, 013003 (2017).
- [47] G. Ganbold, T. Gutsche, M. A. Ivanov, and V. E. Lyubovitskij, *J. Phys. G* **42**, 075002 (2015), [arXiv:1410.3741 [hep-ph]].
- [48] T. Gutsche, M. A. Ivanov, J. G. Körner, V. E. Lyubovitskij, P. Santorelli, and C. T. Tran, *Phys. Rev. D* **98**, 053003 (2018).
- [49] S. Dubnička, A. Z. Dubničková, N. Haby, M. A. Ivanov, A. Liptaj, and G. S. Nurbakova, *Few-Body Syst.* **57**, 121 (2016).
- [50] T. Gutsche, M. A. Ivanov, J. G. Körner, V. E. Lyubovitskij, P. Santorelli, and N. Haby, *Phys. Rev. D* **91**, 074001 (2015).
- [51] T. Gutsche, M. A. Ivanov, J. G. Körner, V. E. Lyubovitskij, and P. Santorelli, *Phys. Rev. D* **87**, 074031 (2013).
- [52] M. A. Ivanov and C. T. Tran, *Phys. Rev. D* **92**, 074030 (2015).
- [53] A. Salam, *Nuovo Cimento* **25**, 224 (1962).
- [54] S. Weinberg, *Phys. Rev.* **130**, 776 (1963).
- [55] Yuanxin Zheng, Zuxin Cai, Gang Li, Shidong Liu, Jiajun Wu, Qi Wu, *Phys. Rev. D* **109**, 014027 (2024).
- [56] N.Brambilla, S.Eidelman, C.Hanhart, A.Nefediev, C.-P.Shen, C. E.Thomas, A.Vairo and C.-Z.Yuan, *Phys. Rep.* **873**, 1 (2020).
- [57] Richard F. Lebed, Ryan E. Mitchell, and Eric S. Swanson, *Prog. Part. Nucl. Phys.* **93**, 143 (2017), [arXiv:1610.04528 [hep-ph]].
- [58] X. L. Wang *et al.* [Belle Collaboration], *Phys. Rev. D* **105**, 112011 (2022), [arXiv:2209.00810 [hep-ex]].
- [59] Stanislav Dubnicka, Anna Z. Dubnickova, Mikhail A. Ivanov, Juergen G. Koerner, Pietro Santorelli, and Gozyl G. Saidullaeva, *Phys. Rev. D* **84**, 014006 (2011), [arXiv:1104.3974v2 [hep-ph]].
- [60] H.-X.Chen, W.Chen, X.Liu, and S.-L.Zhu, *Phys. Rep.* **639**, 1 (2016), [arXiv:1601.02092 [hep-ph]].